Code Predictions Versus Small Scale Bridge Deck Model Test Measurements

PHILIP PERDIKARIS AND MICHAEL PETROU

This paper presents the test results of eight 1/6.6 bridge deck models of an 8.5 in. thick and 50 ft long prototype concrete bridge deck supported on four simply supported steel girders spaced at 7 ft or 10 ft and subjected to a static concentrated wheel-load. The effects of the lateral restraint, girder spacing and amount of reinforcement on the behavior of the deck is determined and discussed. In addition to the enhancement of the ultimate load carrying capacity of the deck, membrane compressive forces present in the deck may shift the primary failure mode from a flexural type to that of punching shear. The effect of this arching action mechanism on the bridge deck response explains the differences between the observed ultimate strength values and the shear strength predictions by the ACI 318 and the European CEB Code. The shear capacity code predictions are conservative (down to about 28% of the measured ultimate strength values). The level of restraint (deck continuity) in a non-composite bridge deck affects the arching action mechanism considerably higher than the amount of reinforcement specified by the AASHTO and Ontario design approach and the girder spacing used in existing highway concrete bridge decks (7 to 10 ft).

The improvement of the current AASHTO design approach for reinforced concrete bridge decks (1) is the major objective of an on-going research project at Case Western Reserve University. Non-composite, reinforced concrete bridge deck models (1/6.6 scale) supported on steel girders are tested under static, fixed pulsating and moving wheel-loads (2 to 4). A prototype girder spacing of either 7 ft or 10 ft (2.13 m or 3.05 m) is assumed corresponding to a lower and upper girder spacing limit, respectively, for highway reinforced concrete bridge decks built in North America. This paper focuses on the effects of reinforcement ratio, girder spacing and lateral restraint on the load-deflection response and failure mode of reinforced concrete highway bridge decks subjected to a static concentrated wheel-load.

The reinforced concrete deck models are tested at nine specified locations to study the influence of the deck continuity level (lateral restraint). The failure mode (flexural or punching shear) for each restraint level and girder spacing is determined. Selected deck panels simply supported on adjacent steel girders are also tested to determine a lower limit of the compressive membrane action which enhances the load-carrying capacity of the decks (5, 6). It is apparent that, although eventually all the decks punched through, the punching shear mode is more prevalent for the orthotropically reinforced decks with girders spaced at 7 ft (2.13 m). For the decks with a girder spacing of 10 ft (3.05 m) failure occurred in a combined flexural-shear type mode. Finally, the ultimate strength values from the physical model tests are compared with the flexural capacity of the deck predicted by the yield-line theory (7) and the shear capacity of the deck predicted by the ACI 318 (8) and the European CEB Code (Comite Euro-International du Beton) (9).

Department of Civil Engineering, Case Western Reserve University, Cleveland, Ohio 44106

BEHAVIOR OF BRIDGE DECKS - DISCUSSION OF MODEL TEST RESULTS

Tests are performed on 1/6.6 scale non-composite concrete deck slab models (see Fig. 1) on steel girders reinforced according to the AASHTO (ρ_t = 0.7% top and bottom transversely and ρ_ℓ = 0.35% top and bottom longitudinally) and the current Ontario Highway Bridge Design Code (ρ = 0.3% top and bottom in both transverse and longitudinal directions)(10). The testing program is presented in Table 1. Only the results of the tests performed under a static load are presented in this paper. The assumed prototype structure is a 50 ft (15.24 m) long, simply supported, non-composite highway bridge with an 8.5 in. (216 mm) thick reinforced concrete deck on four W36x150 steel girders spaced at either 7 ft (2.13 m) or 10 ft (3.05 m). Details regarding the model concrete and steel used and instrumentation can be found in Refs. 2 to 4. The measured ultimate strength values, V_{exp}, of the deck models (B series) subjected to a static concentrated wheel-load with a prototype contact area of 10 in. (longitudinal) x 24 in. (transverse) (254 x 610 mm) are shown in Tables 2 and 3.

The load-deflection curves for all bridge deck models are presented in Fig. 2. The curves with a distinct nearly horizontal plateau, indicating extensive steel yielding and a ductile response, correspond to the deck panels that failed primarily in flexure. All the specimens with a ductile response eventually punched through. The presence of a compressive membrane action in the deck delays the opening of the flexural cracks and stressing of the tension reinforcement. This may shift the primary failure mode from flexural to punching shear. The reinforced concrete deck models that failed primarily in shear exhibited a brittle behavior.

Representative load-deflection curves in terms of non-

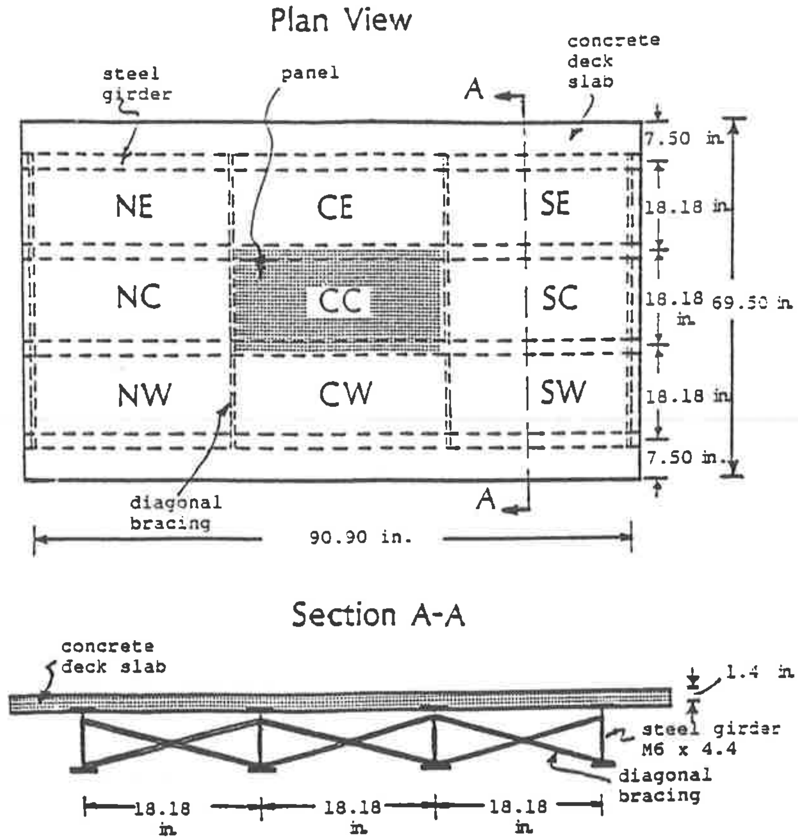

FIGURE 1 Dimensions for the 1/6.6 scale bridge deck model with a prototype girder spacing of 10 ft simply supported over a 50 ft span (1 in = 25.4 mm; 1 ft = 0.3 m).

dimensional parameters are presented in Fig. 3. The applied load to ultimate strength ratio is plotted as a function of the net load-point deck deflection to thickness ratio for two reinforcing patterns (AASHTO and Ontario design), two prototype girder spacings (7 and 10 ft) and two extreme deck boundary conditions (full and no deck continuity). The ultimate net deck deflections never exceeded 50% of the deck thickness. A much narrower peak deflection range of about 0.3h to 0.45h (h = deck thickness) was observed for the isotropically reinforced decks (Fig. 3b) compared to that of 0.08h to 0.46h for the AASHTO deck design (Fig. 3a). The decks reinforced according to the AASHTO Code showed considerably higher influence of girder spacing and lateral restraint on the type of failure mode than in the case of the "Ontario" decks. It is apparent that the response of the lighter reinforced decks (Ontario design), is really independent of girder spacing for prototype values between 7 and 10 ft, at least for the boundary conditions present in non-composite "concrete slab - steel girder" type bridge decks.

The concrete strains on the top deck surface in the transverse direction (perpendicular to the traffic direction) measured next to the loaded area and the steel strains in the transverse tension steel measured at the center of selected deck specimens are presented in Fig. 4 as a function of the applied load to ultimate strength ratio. Results are shown for the simply supported deck panel BO-10S (no deck continuity) and a partially continuous (higher level lateral restraint) deck panel of BO-10C with orthotropic reinforcement (AASHTO) and 10 ft prototype girder spacing. For the concrete strain measurements, data point A (BO-10S) and for the steel strain measurements, data points B (BO-10S) and C (BO-10C) correspond to the largest strain values recorded before the malfunction of the gages. The shape of the load-strain curves, the peak compressive concrete strain value and the load level at which concrete strain peaks and reinforcement yields are closely related to the mechanics of the arching mechanism and the type of failure mode. As indicated in Fig. 4, in the case of BO-10C (punching shear mode rather dominant) the top transverse concrete strain measured next to the applied load peaks closer to the ultimate load level with a lower peak value than that measured in specimen BO-10S, where the primary mode of failure is flexural. Initially, both top surface concrete and bottom steel strains increase at more or less the same rate up to the first flexural cracking. Beyond this point, the transverse tension steel strains at the bottom of the deck increase much faster than the compressive concrete strains at the top of the deck (neutral axis moves upwards). It is important to note that while the transverse tension steel starts yielding (at 2000 to 2500 $\mu\epsilon$) the rate of increase in the transverse concrete strain

TABLE 1 EXPERIMENTAL PROGRAM FOR THE 1/6.6 SCALE BRIDGE DECK MODEL SPECIMENS WITH A GIRDER SPACING OF 10 AND 7 ft (1 psi = 6.9 kPA; 1 in = 25.4 mm)

Deck Model	Boundary Cond.	h (in.)	Reinforcing Pattern	Number of Static Load Tests	Average Compressive Strength, f'_c (psi) (2 x 4 in. Cyl.)
BI-10C	cont.[a]	1.40[c]	isotropic[d]	6	7,259
BO-10C	cont.	1.40	orthotropic[e]	6	7,011
BI-10S	s.sup.[b]	1.40	isotropic	1	6,497
BO-10S	s.sup.	1.40	orthotropic	1	6,907
BI-7C	cont.	1.30	isotropic	5	6,685
BO-7C	cont.	1.30	orthotropic	5	5,783
BI-7S	s.sup.	1.30	isotropic	1	6,917
BO-7S	s.sup.	1.30	orthotropic	1	6,917

Notes:

[a] cont. = continuous bridge deck model (see FIGURE 1)

[b] s.sup.= simply supported deck panel model (see FIGURE 1)

[c] h = deck thickness

[d] ρ_ℓ = 0.003 and ρ_t = 0.003 (top and bottom)-Ontario design

[e] ρ_ℓ = 0.0035 and ρ_t = 0.007 (top and bottom)-AASHTO design

(ℓ = longitudinal; t = transverse)

TABLE 2 STATIC ULTIMATE STRENGTH OF CONTINUOUS BRIDGE DECK MODELS (1 lb = 4.45 N)

Deck Model	Ultimate Strength of Each Panel (lb)								Average Ultimate Strength (lb)
	NW	NC	NE	CW	CC	CE	SC	SE	
BI-10C[1]	-	5,994	5,200	-	7,600	6,079	5,188	5,125	5,864
BO-10C[1]	-	8,289	7,751	-	10,608	9,009	8,350	7,397	8,567
BI-7C[2]	8,514	8,070	8,563	-	8,858	7,874	-	-	8,376
BO-7C[3]	-	-	11,811	13,091	16,142	-	13,484	12,106	13,327

Note:

Sequence of testing:
1. CC - NC - CE - NE - SC - SE
2. NE - CE - NW - NC - CC
3. NE - SE - SC - CW - CC

TABLE 3 STATIC ULTIMATE STRENGTH OF SIMPLY SUPPORTED DECK PANEL MODELS (1 lb = 4.45 N)

Deck Model	Ultimate Strength (lb)
BI-10S	3,934
BO-10S	5,350
BI-7S	4,761
BO-7S	6,885

decreases and eventually it may even decrease. This means that as the ultimate strength level is approached the compressive resultant force carried by the concrete is decreasing and therefore a compressive membrane force should exist for equilibrium to be satisfied.

For a constant loaded area and deck thickness, the arching action mechanism in the deck, and as a result its load-deflection response and failure mode, is affected by the amount of reinforcement, girder spacing (deck slenderness) and lateral restraint. The lateral restraint is provided by the part of the deck slab surrounding the loaded area and by the deck supports.

Reinforcement ratio

The amount of reinforcement for an orthotropically reinforced deck panel (AASHTO design) is 130% and 17% higher in the transverse and longitudinal direction, respectively, than for an isotropically reinforced deck panel (Ontario design). The ratio of the measured ultimate strength values to the yield-line theory predictions, V_{exp}/V_J, are shown in Fig. 5 for both AASHTO and Ontario designs and different boundary conditions. The three levels of continuity C0, C1 and C2 correspond to the cases of a simply supported panel, an edge panel and a central panel of the continuous deck slab, respectively. As indicated in Fig. 5, while for the orthotropically reinforced decks (BO-10) the observed ultimate strength ranges between 1.4 (simply supported) and 2.7 (central panel of BO-10C) times the Johansen load (assuming a concentrated applied load), for the isotropically reinforced deck (BI-10) varies between 1.7 (simply supported) and 3.3 (central panel of BI-10C) times the Johansen load. The bottom reinforcement ratio for values equal to or higher than 0.3% seems to have a very small effect on the arching action for specimens with a span to thickness ratio equal to 13 (prototype girder spacing of 10 ft and deck thickness of 8.5 in.). In the case of a span to thickness ratio of about 9 (prototype girder spacing of 7 ft and deck thickness of 8.5 in.) the effect of reinforcement on the effectiveness of the arching mechanism is even smaller.

Girder spacing (deck slenderness)

The load-carrying capacity of all deck models increased with decreasing slenderness, as shown in Fig. 2. The effect of slenderness on the deck's ultimate deflection is considerably higher for the orthotropically reinforced model decks (AASHTO design), as can be seen in Fig. 2. As shown in Fig. 5, the influence of girder spacing on the enhancement of the deck's ultimate strength due to the arching mechanism is considerable, especially for those decks designed according to the current AASHTO Code. The fully restrained deck panels (central panel) with a prototype girder spacing of 7 ft (2.13 m) exhibited a load-carrying capacity increase over the Johansen load of about 2.2 and 1.5 times that measured in similarly restrained deck panels supported on steel girders spaced at 10 ft (3.05 m) for the AASHTO and Ontario design, respectively.

Lateral restraint

It is clear from Fig. 5 that the arching action mechanism becomes more prevalent with increasing rotational and translational transverse restraint in the deck. It appears that the enhancement of the deck's load carrying capacity is more sensitive to increasing lateral restraint for the AASHTO than the Ontario design independently of the girder spacing. The degree of influence of deck continuity on the arching action for the two reinforcing patterns (AASHTO and Ontario design) is considerably higher compared to the influence of girder spacing and amount of reinforcement.

CODE PREDICTIONS VS. TEST RESULTS

The ratio of the measured load-carrying capacity, V_{exp}, to the nominal shear strength according to the ACI 318 (1989) Code,

$$V_{ACI} = (2 + 4/\beta_c)\ b_o d\sqrt{f_c'} \leq 4\, b_o d\sqrt{f_c'} \text{ (lb)} \qquad (1)$$

where the cylinder compressive strength of concrete f_c' is

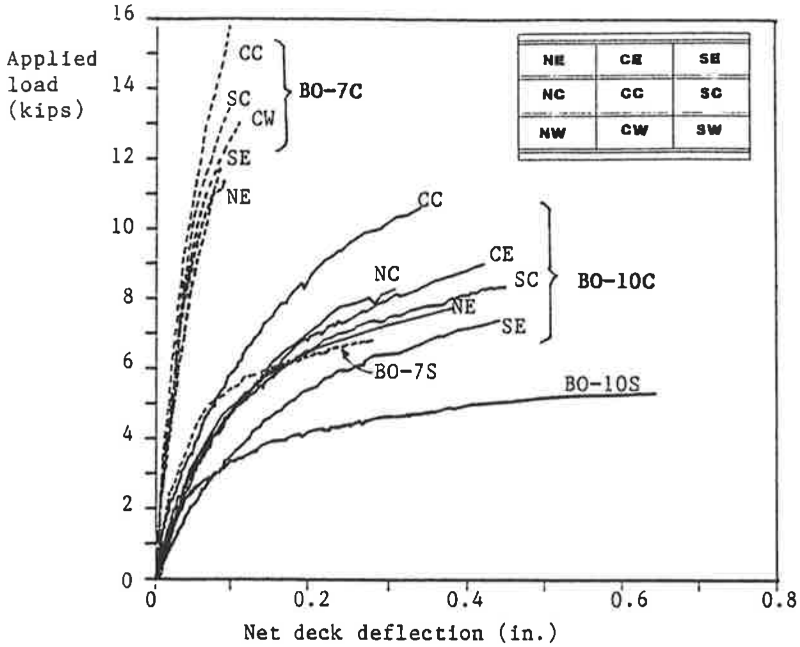

a) Orthotropic reinforcement (AASHTO design).

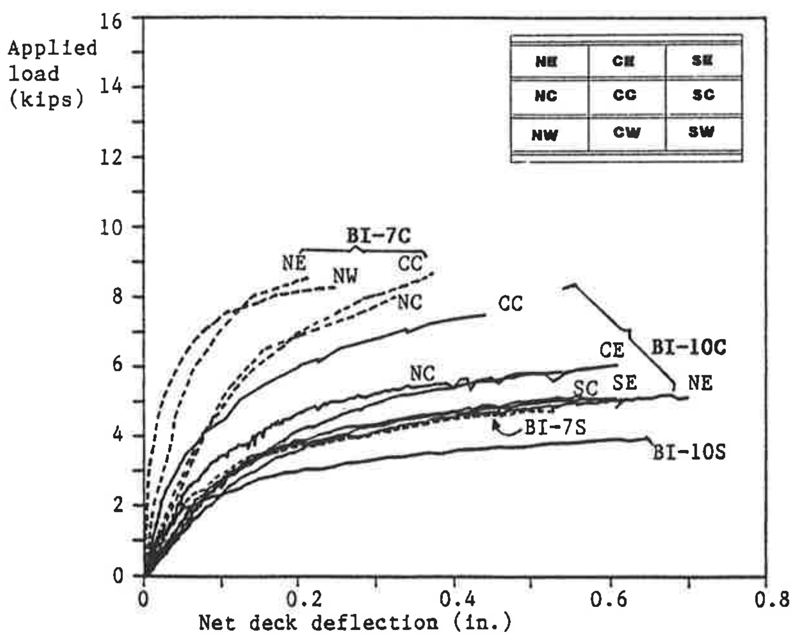

b) Isotropic reinforcement (Ontario design).

FIGURE 2 Experimental load-deflection curves under a static concentrated wheel-load for the 1/6.6 scale model bridge decks (girder spacing of 7 and 10 ft).

in psi, $\beta_c = 2.4$ is the ratio of the long-to-short side of the loaded area and b_o (in.) the perimeter of the critical section equal to the perimeter of the load area plus four times the effective depth d (in.), is shown in Fig. 5. Eq. 1 is unable to predict the shear capacity of laterally restrained slabs. It takes into account only the compressive strength of concrete, effective depth of the deck and the assumed perimeter of the critical section. The compressive membrane action enhances not only the flexural capacity of the deck but also its shear capacity. Hence, the ultimate strength of a highly restrained deck such as BO-7C, is considerably greater than the ACI Code shear strength prediction, as can be seen in Fig. 5. The ultimate strength of all panels for the isotropically reinforced deck model BI-10C (except that of the central panel CC) and all the non-continuous deck panels (simply supported) are very close to the ACI Code predictions (see Fig. 5). These specimens appear to have failed in flexure.

The shear resistance of a reinforced concrete slab according to the European CEB-FIP 1990 Model Code is

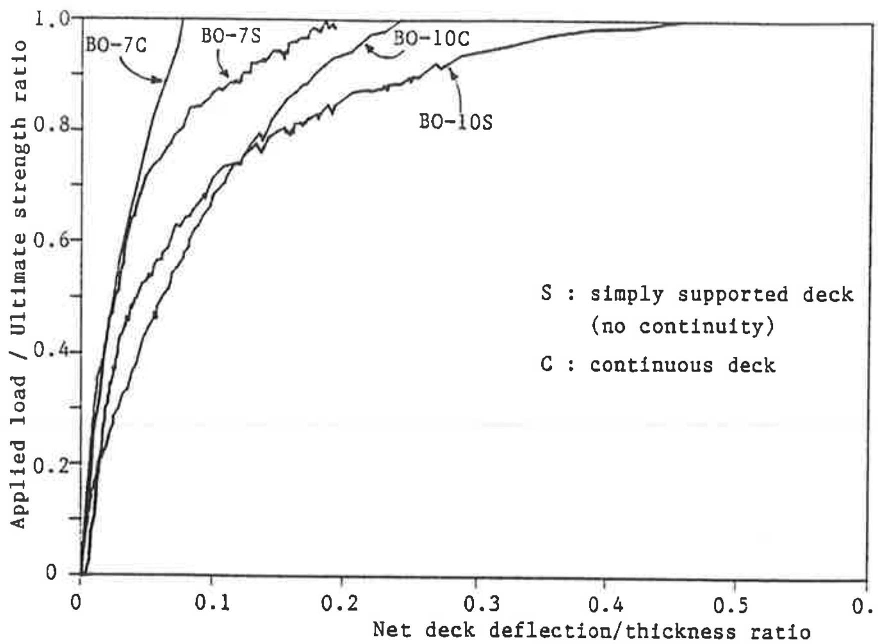

a) **Orthotropic reinforcement (AASHTO design).**

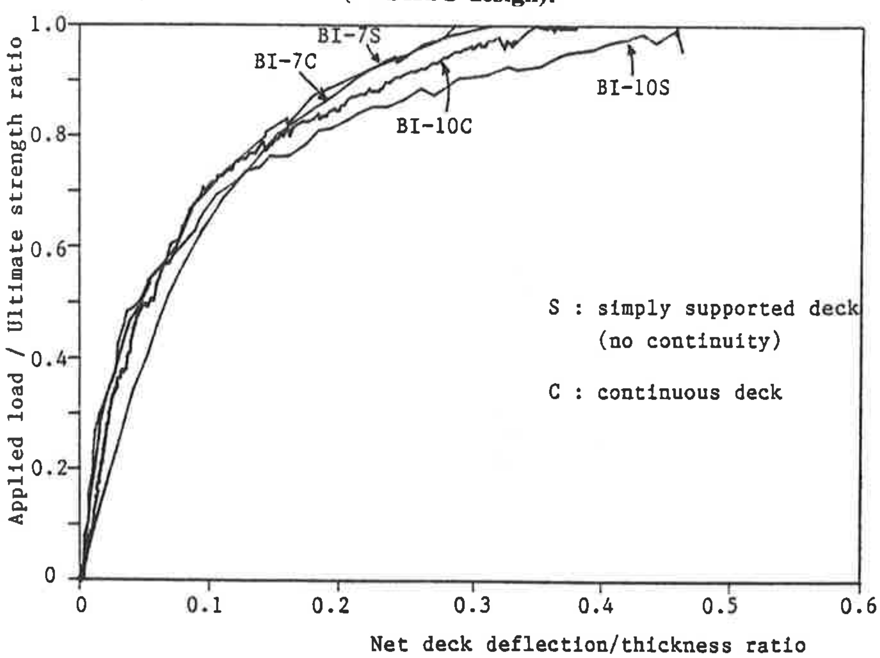

b) **Isotropic reinforcement (Ontario design).**

FIGURE 3 Non-dimensional load-deflection curves under a static concentrated wheel-load for two levels of deck continuity (S and C) and two girder spacings (7 and 10 ft).

given by the equation

$$V_{CEB} = 0.12\,\xi\,(100\,\rho f_{ck})^{1/3}\,ud \quad (N) \qquad (2)$$

where $\xi = 1 + \sqrt{200/d}$ (d in mm), u (in mm) is the perimeter of the critical section equal to the perimeter of the load area plus $4\pi d$(mm), ρ the average reinforcement ratio in the two orthogonal directions and f_{ck} the characteristic cylinder compressive strength of concrete (MPa). The CEB-FIP Model Code takes into account the effect of the flexural reinforcement on the shear capacity of the deck slab but it does not consider other important parameters, such as lateral and rotational restraint in the deck and deck slenderness. The CEB predictions, at least for the parameter values studied, appear to be either very similar to or slightly more conservative than the ACI predictions. For all non-continuous deck panels (simply supported) both ACI and CEB codes give predictions very close to the experimental findings, as expected,

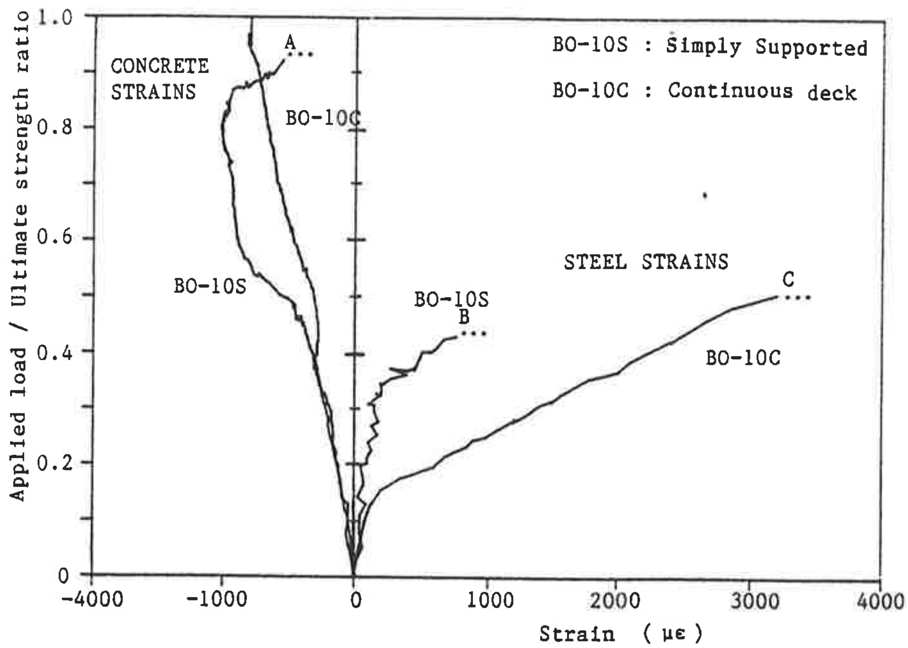

FIGURE 4 Measured transverse steel and concrete strain at the bottom midspan rebar and top deck surface next to the loaded area, respectively, for two levels of deck continuity (S and C) and a girder spacing of 10 ft as a function of the level of applied load.

independently of girder spacing and reinforcing pattern.

CONCLUSIONS

1. A given level of lateral restraint in the deck for the Ontario design has a higher influence on the effectiveness of the arching mechanism in enhancing its ultimate strength above the Johansen load than for the AASHTO design.
2. The enhancement of the deck's load carrying capacity appears to be more sensitive to increasing lateral restraint for the AASHTO than the Ontario design independently of the girder spacing.
3. At least for girder spacings between 7 and 10 ft and deck thickness of 8.5 in. (deck slenderness between 9 and 14) the level of lateral and rotational restraint (deck continuity) in a non-composite bridge deck affects the arching action mechanism considerably more than the decrease of girder spacing (from 10 ft to 7 ft) or increase of reinforcement (adopting AASHTO vs. Ontario design).
4. Although some of the decks, such as those designed according to the Ontario Design Code and supported on girders spaced at 10 ft, failed primarily in flexure, all of the decks eventually punched through with a maximum net deflection always less than 50% of the deck thickness. Those decks designed according to the AASHTO code (with either 7 or 10 ft girder spacing) exhibited a rather brittle response and a primary failure mode of punching shear.
5. The CEB-FIP (1990) shear strength predictions are either very similar to or slightly more conservative than the ACI predictions.
6. For all non-continuous deck panels (simply supported) both ACI and CEB codes give predictions very close to the experimental findings independently of girder spacing and reinforcing pattern.
7. Both ACI and CEB codes are more conservative in the case of decks with isotropic reinforcement (Ontario design).

ACKNOWLEDGMENTS

The model tests for highway bridge decks were performed at the Structures Laboratory of Case Western Reserve University. Aidong Wang, graduate research assistant in the Department of Civil Engineering, has performed part of the experimental work presented. Funding for this research program was provided by the Ohio Department of Transportation (ODOT) and the Federal Highway Administration. Any opinions, findings and conclusions expressed in this paper are those of the writers and do not necessarily reflect the views of ODOT and FHWA.

REFERENCES

1. AASHTO Standard Specification of Highway Bridges (1989), 14th Ed., American Association of State Highway and Transportation Officials, Washington, D.C.
2. Perdikaris, P.C., and Beim, S. (1986), "R/C Bridge Decks Under Pulsating and Moving Load," Journal of Structural Engineering, ASCE, 114(3), March, pp. 591-607.

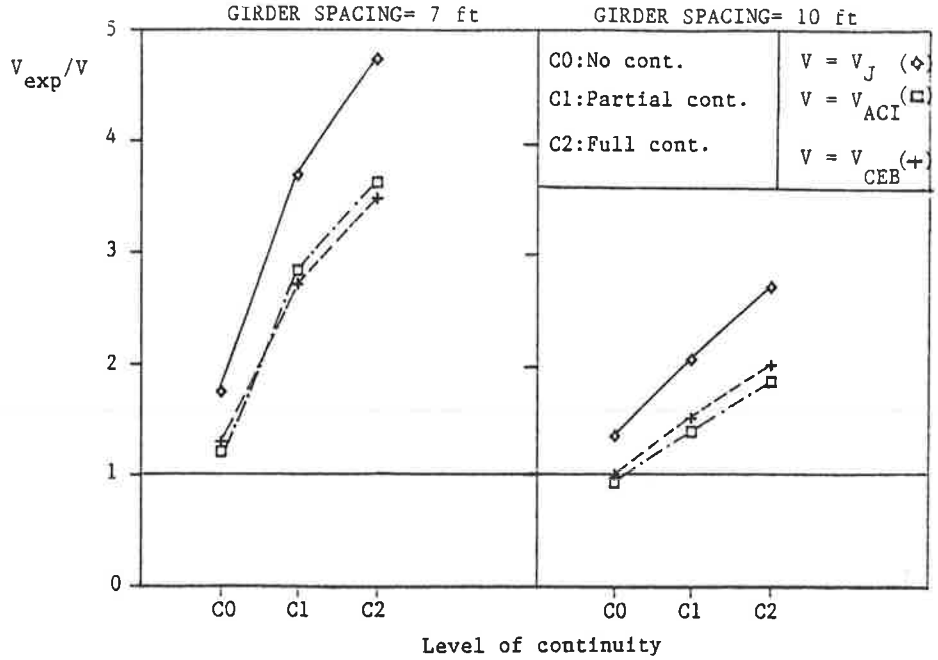

a) Orthotropic reinforcement (AASHTO design).

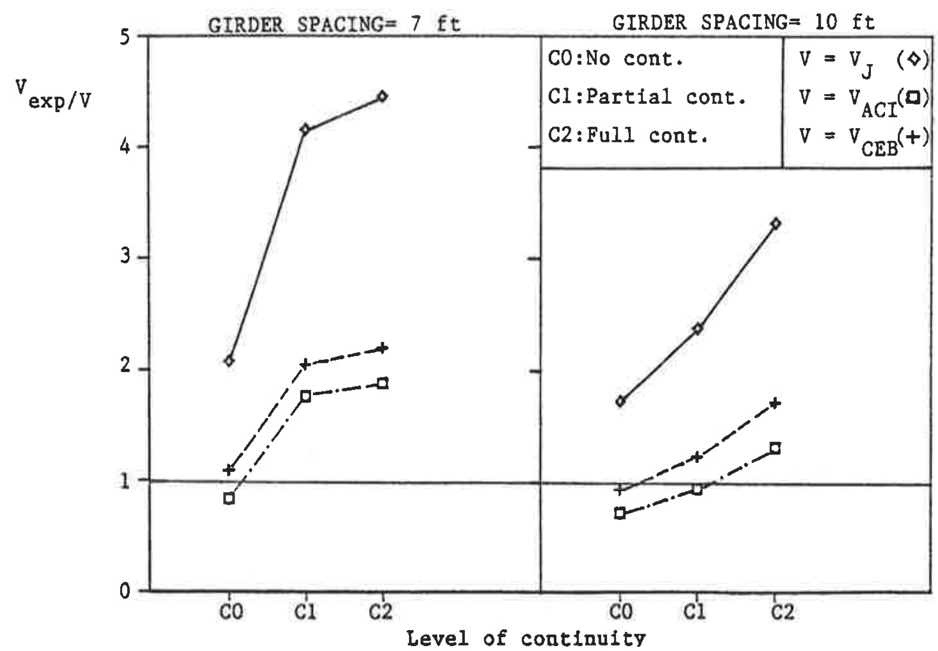

b) Isotropic reinforcement (Ontario design).

FIGURE 5 Comparison of experimental static ultimate strength values with yield-line theory and ACI, CEB code predictions.

3. Perdikaris, P.C., Beim, S., and Bousias, S. (1989), "Slab Continuity Effect on Ultimate and Fatigue Strength of R/C Bridge Deck Models," ACI Structural Journal, 86(4), July-August, pp. 483-491.
4. Petrou, M.F., and Perdikaris, P.C. (1990), "Small Scale Model Tests: Arching Action in Reinforced Concrete Bridge Decks;" 3rd International Conference on Short and Medium Span Bridges, Toronto, Canada, August.
5. Hewitt, B.E., and Batchelor, B. deV. (1975), "Punching Shear Strength of Restrained Slabs," Journal of the Structural Division, ASCE, 101(ST9), pp. 1837-1853.
6. Csagoly, P., Holowka, M., and Dorton, R. (1978), "The True Behavior of Thin Concrete Bridge Slabs," Transportation Research Record No. 664, Transportation Research Board, pp. 171-179.
7. Johansen, K.W. (1962), Yield-line Theory, Cement and Concrete Association, London.
8. ACI Committee 318 (1989), "Building Code Requirements for Reinforced Concrete and Commentary," American Concrete Institute, Detroit,

Michigan.
9. CEB-FIP Model Code (1990), First Draft, Bulletin No. 196, Comite Euro-Internationale du Beton, Lausanne, Switzerland, September.
10. Ontario Highway Bridge Design Code (1983), 2nd Ed., Highway Engineering Division, Ontario Ministry of Transportation and Communications, Downsview, Ontario, pp. 357.